American Mineralogist, Volume 83, pages 577–589, 1998

Crystal chemistry of the zeolites erionite and offretite

E. Passaglia,[1] G. Artioli,[2,*] and A. Gualtieri[1]

[1]Dipartimento di Scienze della Terra, Università di Modena, via S. Eufemia 19, I-41100 Modena, Italy
[2]Dipartimento di Scienze della Terra, Università di Milano, via Botticelli 23, I-20133 Milano, Italy

Abstract

Many known occurrences of the zeolites erionite and offretite have been characterized by electron probe microanalysis, X-ray powder diffraction, and optical microscopy. For the first time, a substantial amount of experimentally consistent and homogeneous chemical and crystallographic data have been evaluated for these natural zeolites. Systematic analysis of the data, performed by statistical multivariate analysis, leads to the following conclusions: (1) the two zeolites have well-defined compositional fields in the chemical space describing the extraframework cation content, best illustrated in a Mg-Ca(+Na)-K(+Sr+Ba) diagram; (2) no discrimination is possible on the basis of the framework Si/Al ratio because of the extensive compositional overlap between the two species, however the Si-Al content in the framework tetrahedra is the major control on the unit-cell volume dimensions, particularly in erionite; (3) the crystal chemistry of the Mg cations is a major factor in controlling the crystallization of the mineral species; (4) cation compositions at the boundary of the recognized compositional fields might be due to chemical averaging of two-phase intergrowths, although these mixed-phase occurrences are much less common than previously thought; (5) the sign of optical elongation is not a distinctive character of the two phases, it is related to the Si/Al ratio in the framework tetrahedra of each zeolite type and cannot be used for identification purposes; (6) the zeolite mineral species epitaxially overgrown on levyne in all cases is identified as erionite; in a few cases offretite was found to be overgrown on chabazite; (7) erionite samples epitaxially overgrown on levyne are substantially more Al-rich and Mg-poor than the erionite samples associated with other zeolites.

Introduction

Erionite and offretite are natural zeolites having different topologies ([ERI]- and [OFF]-topological codes following Meier and Olson 1992). Both zeolites are found in vugs of volcanic massive rocks, and available literature descriptions include: one-phase occurrences and epitaxial intergrowths of the two species (Pongiluppi 1976; Rinaldi 1976; Wise and Tschernich 1976; Hentschel and Schricke 1976; Betz and Hentschel 1978; Rychlý et al. 1982), epitaxial overgrowth of both erionite and offretite on levyne (Shimazu and Mizota 1972; Passaglia et al. 1974; Sheppard et al. 1974; Wise and Tschernich 1976; England and Ostwald 1979; Birch 1989; Kile and Modreski 1988), and epitaxial overgrowth of offretite on chabazite (Passaglia and Tagliavini 1994; Passaglia et al. 1996). Only erionite is also found as an authigenic mineral in volcanoclastic silicic layers and tuffs diagenetically altered in continental (Staples and Gard 1959; Sheppard and Gude 1969; Sheppard et al. 1965; Gude and Sheppard 1981; Boles and Surdam 1979; Surdam and Eugster 1976) and marine (Shameshima 1978) environments. Given the wider range for conditions of formation, erionite is the more common of the two mineral zeolites, whereas offretite occurrences are scarce. Typical occurrences, morphological and optical features, and earlier crystal chemical studies are well described in the literature (Sheppard and Gude 1969; Wise and Tschernich 1976; Gottardi and Galli 1985; Tschernich 1992). The present study stems from two major problems commonly encountered in the characterization of erionite-offretite mineral samples: (1) The identification of mineral species is troublesome, due to the structural and crystal chemical similarities of the two zeolites; and (2) the literature descriptions available to date do not provide clear discriminatory parameters for the definition and the distinction of the two minerals, unless a complete structural study is performed.

The first point is readily justified: In the literature it is possible to find several cases where the minerals were misidentified by simple routine mineralogical analysis. An example is the sample from Beech Creek, Oregon, which was originally identified as an offretite overgrowth on levyne on the basis of optical elongation sign and X-ray powder diffraction data (Sheppard et al. 1974), but was subsequently redefined as erionite on levyne on the basis of thorough X-ray and electron diffraction analysis and adsorption capacity measurements (Bennett and Grose

* E-mail: artioli@iummix.terra.unimi.it

0003–004X/98/0506–0577$05.00

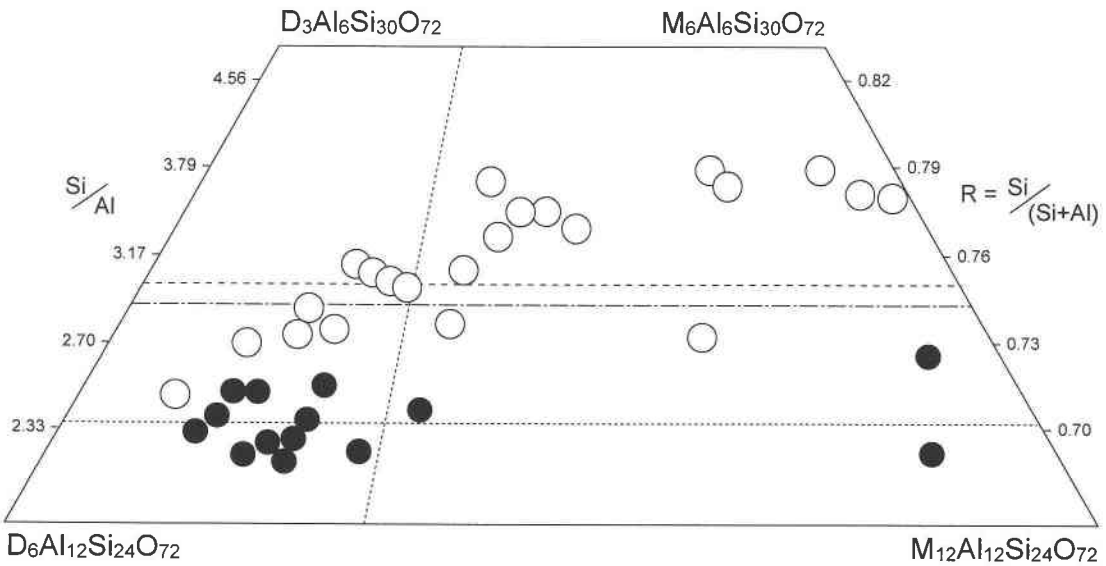

FIGURE 1. Compositional diagram showing the reliable chemical analyses of erionite (open circles) and offretite (solid circles) from the literature. Sources of the data: Batiashvili and Gvakhariya (1968); Belitskiy and Bukin (1968); Birch (1988, 1889); Boles and Surdam (1979); England and Ostwald (1979); Gude and Sheppard (1981); Harada et al. (1967); Kile and Modreski (1988); Noh and Kim (1986); Passaglia et al. (1974); Passaglia and Tagliavini (1994, 1995); Pongiluppi (1976); Rinaldi (1976); Rychlý et al. (1982); Sameshima (1978); Sheppard et al. (1965); Sheppard and Gude (1969); Staples and Gard (1959); Surdam and Eugster (1976), Wise and Tschernich (1976). About half of the erionites are reported to be "hydrothermal," and half are sedimentary. M = (Na + K); D = (Ca + Mg + Sr + Ba). All data normalized to 72 framework O atoms. Horizontal discrimination lines based on Si/Al ratio are after Sheppard and Gude (1969) [–·–·–], Wise and Tschernich (1976) [- - - -], and Rinaldi (1976) [·····]. Sub-vertical line (D = M) is the discriminant after Sheppard and Gude (1969).

1978). Several of the samples obtained for the present study were also misidentified by the original authors: The close relationship between the crystal structures of the two minerals (Bennett and Gard 1967) is the cause for such frequent misidentifications. Although both crystal structures are now reasonably well defined, at least in terms of major crystallographic features (Staples and Gard 1959; Kawahara and Curien 1969; Gard and Tait 1972, 1973; Alberti et al. 1996; Gualtieri et al. 1998), the available crystal chemical characterizations are incomplete and often inconsistent. This is the cause of the second problem listed above: Based on the present literature, it is impossible to define universal discrimination criteria applicable to all reported erionite and offretite samples.

Problems exist because earlier discrimination parameters were based on a limited number of samples. Sheppard and Gude (1969) proposed species distinction based on the optical sign of elongation (positive in erionite, negative in offretite, a widely used identification parameter in subsequent studies) and on chemical parameters [erionite: Si/(Al + Fe) > 2.9 and (Na + K) > (Ca + Mg)]. Subsequently, Wise and Tschernich (1976) and Rinaldi (1976) proposed a distinction based on the Si/Al ratio, the former defining as erionite the mineral having Si/Al > 3.0, the latter defining as erionite the mineral having Si/Al > 2.4.

If all reliable chemical analyses of erionites and offretites available in the literature are inserted in a discriminatory diagram based on the above chemical parameters (Fig. 1), it is evident that none among the proposed criteria satisfactorily defines appropriate compositional fields apt to describe the literature information. Chemical analyses are considered to be reliable if (Si + Al) ≈ 36, on the basis of 72 O atoms; and balance error E ≤ 10%, where E% (Passaglia 1970) is

$$100 \times [(Al + Fe)_{ob} - Al_{th}]/Al_{th} \quad (1)$$

$$Al_{th} = Na + K + 2 \times (Ca + Mg + Sr + Ba). \quad (2)$$

The situation is even more confused if we try to plot the available data describing the extraframework cation content of the two zeolites, using the same literature sources (Fig. 2). We assume that the lack of discriminatory compositional fields for the two zeolites is due to several factors: First of all, several minerals in the literature could be simply misidentified; second, several of the analyses may have been carried out on mixed-phase samples.

The present work attempts to redefine the crystal chemistry of erionite and offretite minerals. We collected as many available samples as possible from different localities, identified the associated minerals, and eventually separated pure erionite and offretite samples. For each sample, we performed electron microprobe analysis (EMPA), thermal gravimetric analysis, X-ray powder diffraction, and optical microscopy. Statistical analysis of

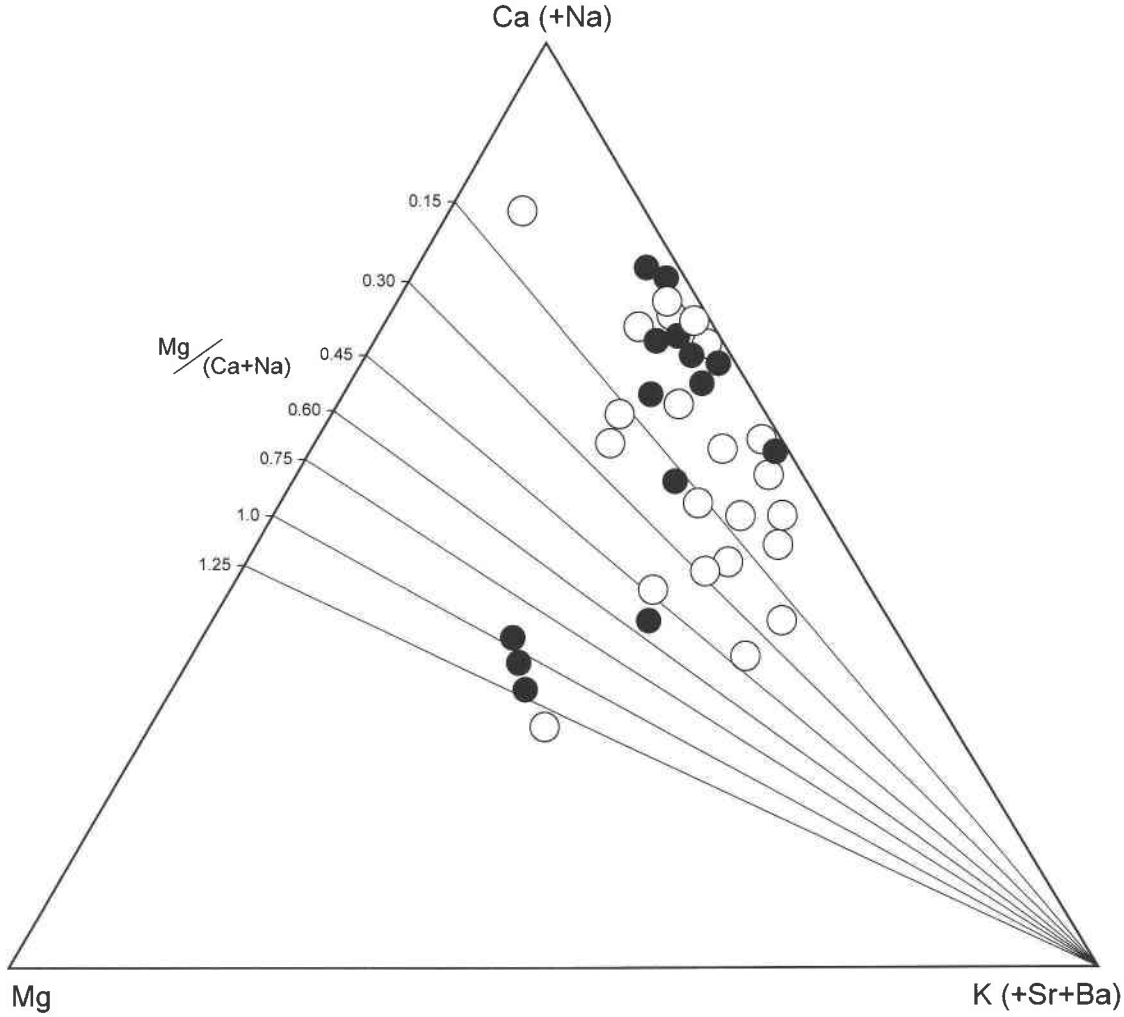

FIGURE 2. Compositional diagram showing the extraframework cation content of reliable chemical analyses of erionite and offretite minerals in the literature. Sources of the data and symbols as in Figure 1.

the internally consistent and homogeneous chemical and crystallographic data was used to evaluate and interpret possible discrimination parameters between the two zeolites. A companion study (Gualtieri et al. 1998) presents the full structural characterization of a limited number of samples to establish a relationship between crystal chemistry and crystal structure in the two closely related zeolites.

SAMPLE PREPARATION AND IDENTIFICATION

After preliminary screening, 25 erionite and 13 offretite samples were selected, mainly on the basis of our ability to separate a sufficient amount of pure material for all subsequent analyses. Localities and available literature descriptions are reported in Table 1.

Each sample was first checked by optical microscopy to describe the morphological habit and mineral association of the erionite and offretite candidate crystals. A few crystals or crystal aggregates were then hand separated for preliminary X-ray diffraction analysis by long exposures (up to 24 h) using a Gandolfi camera. The nondestructive technique allowed identification of the separated crystals and guaranteed integrity of the crystals for the subsequent EMPA.

Erionite and offretite have very similar X-ray diffraction patterns, due to their similar structures and unit-cell parameters (Kerr et al. 1970; Bennett and Grose 1978). Indeed, careful analysis of the X-ray diffraction patterns is necessary for proper identification of the phases. Most of the Bragg peaks of the two zeolites coincide exactly in the diffraction pattern, apart from a few relatively strong diffraction lines due to the unit-cell doubling in erionite (namely the 101, 201, 211, 213, 311 reflections). This is commonly considered an appropriate test only for the presence of erionite: That is if the lines are absent, then the sample can be considered pure offretite; if the lines are present, this is no guarantee of the absence of offretite in the erionite sample. However, simulation

TABLE 1. Localities of the erionite and offretite samples studied in the present work

No.	Locality	Reference
	erionite	
1	Bog Hill Quarry, Northern Ireland	Foy, pers. comm.
2*	Dunseverick, Northern Ireland	ibid
3*	Ballyclare, Northern Ireland	ibid
4*	Lady Hill Quarry, Northern Ireland	ibid
5	Agate Beach, Oregon, U.S.A.	Wise and Tschernich 1976
6*	Westwold, British Columbia, Canada	ibid
7*	Jindivick, Australia	Birch 1987
8*	Phillip Island, Australia	Birch 1988
9*	Phillip Island, Australia	ibid
10*	Merriwa, Australia	England and Ostwald 1979
11*	Cairns Bay, Australia	Birch 1988
12	Shourdo, Georgia	Batiashvili and Gvakhariya 1968
13	Nizhnyaya Tunguska, Russia	Belitski and Bukin 1968
14*	Beech Creek, Oregon, U.S.A.	Sheppard et al. 1974
15*	Montecchio Maggiore, Italy	Giovagnoli and Boscardin 1979
16	Montecchio Maggiore, Italy	Saccardo, pers. comm.
17*	Montresta, Nuoro, Italy	Passaglia et al. 1974
18	Faedo, Vicenza, Italy	Passaglia and Tagliavini 1995
19†	Araules, Ht. Loire, France	Pongiluppi 1976
20	Ortenberg, Germany	Hentschel 1986
21*	Island of Skye, Scotland	Rinaldi, pers. comm.
22	Campbell Glacier, Antarctica	Vezzalini et al. 1994
23	Mt. Adamson, Antarctica	ibid
24*	Mt. Admason, Antarctica	ibid
25	Durkee, Oregon, U.S.A.	Sheppard and Gude 1969
	offretite	
1	Germany	Gabelica, pers. comm.
2	Contrada Re, Vicenza, Italy	Boscardin, pers. comm.
3	Punta del Hattaral, Spain	Gabelica, pers. comm.
4	Sasbach, Germany	Rinaldi 1976
5	Horseshoe Dam, Arizona, U.S.A.	Wise and Tschernich 1976
6	Vinarice, Czech Republic	Gabelica, pers. comm.
7	Herbstein, Germany	Hentschel 1980
8	Gedern, Germany	Betz and Hentschel 1978
9	Mont Semiol, France	Passaglia and Tagliavini 1994
10	Adamello, Italy	ibid
11	Fittà, Soave, Italy	Passaglia et al. 1996
12	Fittà, Soave, Italy	ibid
13	Montorso Vicentino, Italy	Boscardin, pers. comm.

Note: Available reference information is reported.

* Erionite overgrowth on levyne.

† This sample was originally defined as offretite (Pongiluppi 1976), preliminarily interpreted here as erionite on the basis of X-ray powder diffraction and chemical analysis (which showed that the sample lies on the boundary of the erionite field), and finally shown to be an offretite with a high density of erionite faults by transmission electron microscopy (Gualtieri et al. 1998).

methods based on the structure models of the two phases show that the intensity ratio of Bragg peaks containing only the erionite scattering contribution to those containing both the erionite and the offretite contributions can be used to determine the offretite content in erionite. Figure 3 shows a portion of the simulated X-ray powder diffraction pattern for Cu$K\alpha$ radiation in the angular range 18–22 °2θ. The patterns have been normalized to the intensity of the 210 reflection, to clearly show the change in the 210/211 intensity ratio as a function of the erionite and offretite content of the mineral mixture.

This technique, employing Rietveld analysis based on established structure models, is more than adequate to discriminate among the phases present in the specimen. The only ambiguous case is the sample from Araules, France, see note in Table 1. The method can be readily applied to various powder diffraction patterns, including those obtained by conventional parafocusing diffractometers if abundant material is available or those obtained by optical scanning of Gandolfi films (Lutterotti et al. 1996), in case available material is scarce. Both techniques were used in the present study. Simulations and preliminary semi-quantitative analysis were performed using the GSAS program system (Larson and Von Dreele 1996).

Samples were carefully screened for phase purity and then prepared for subsequent analyses. Usually 4–5 grains or fiber aggregates were enclosed in epoxy resins and polished for electron microprobe analysis; 5 mg of powder were used for thermal gravimetric analysis; and about 20–30 mg of powder were mixed with reagent grade $Pb(NO_3)$ as an internal standard for X-ray diffraction unit-cell parameter measurement. For some samples, especially those showing erionite-levyne intergrowths, it was impossible to separate substantial quantities of pure material. In such cases the pure hand-separated grains were used for chemical analyses, and the impure material was used for the X-ray powder data collection. A multiphase Rietveld analysis was used to extract lattice parameters from these mixed-phase samples.

EXPERIMENTAL METHODS

Chemical analysis

EMPA were performed on an ARL-SEMQ instrument using wavelength dispersive mode of operation, 30 μm diameter electron beam size, 15 kV accelerating voltage, and 20 nA probe sample current. Reference standards were microcline (K), anorthite (Ca), albite (Na, Si, Al), olivine (Fe), diopside (Mg), Sr-anorthite (Sr), and celsian (Ba).

Individual point analyses for each sample ranged from 6 to 27, depending on the number of single grains available in the epoxy mount. In elongated crystals or crystal aggregates, at least 3–4 point analyses were performed along the fiber to check for chemical homogeneity. The point analyses of each sample were highly consistent, showing a variation of major elements within 3% of the estimated instrumental errors and indicating a high degree of chemical homogeneity within each sample. Most EMPA results also proved very reliable in terms of formula stoichiometry (Si + Al = O/2) and charge balance ($E \leq \pm 10\%$). The small variance and the good internal consistency of the single analyses support the assumption that the unit formulae reported in Tables 2 and 3, and resulting from the average of the single point analyses, are representative of the crystal chemistry of each zeolite sample.

The H_2O content has been independently measured by thermal gravimetric analysis (TGA) on all samples for which 5 mg of material were available. When the material was insufficient, the H_2O content was assumed as the weighted average of the measured estimates on other

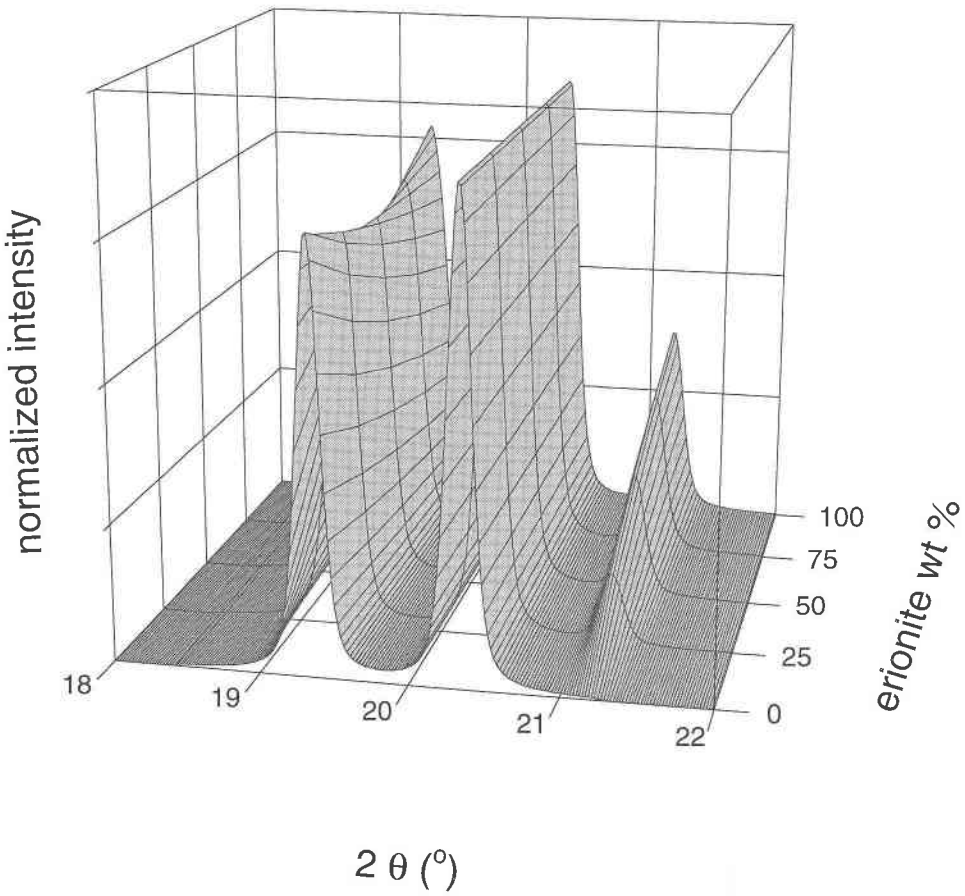

FIGURE 3. Simulation of a portion of the X-ray powder diffraction pattern produced by a mixture of erionite and offretite, as a function of the varying composition of the multi-phase mixture. Intensities were normalized to the 210 Bragg peak.

samples of the same phase. TGA measurements were performed in air on a Seiko SSC/5200 thermoanalyzer, using a heating rate of 10 °C/min.

The chemical analyses reported in Tables 2 and 3 are the EMPA results, renormalized by the H_2O content measured (or estimated) by the TGA analysis. The tables also list the observed optical sign of elongation, as observed with polychromatic polarized light using a gypsum retardation slab (1st order red shift = 550 μm).

Unit-cell parameters measurement

If more than 15–20 mg of sample were available, powder diffraction data were collected on a Philips diffractometer in flat-plate Bragg-Brentano geometry, equipped with a diffracted-beam graphite crystal analyzer. Data were collected using Cu$K\alpha$ radiation in the 5–80 °2θ angular range, fixed steps of 0.03 °2θ and 3 s/step measuring time.

If the available material was less than a few milligrams, data collection was performed in Debye-Scherrer geometry using a Gandolfi camera and Ni-filtered Cu$K\alpha$ radiation. The films were exposed for about 24 h and then scanned by a computer-interfaced OET AS-880 microphotometer. The powder patterns were corrected for film saturation and non-linear response before Rietveld analysis (Lutterotti et al. 1996).

In all instances, the erionite or offretite sample was mixed with reagent grade $Pb(NO_3)_2$ as an internal standard, in the proportion of about 8 wt% of the final mixture. The unit-cell parameter of the lead nitrate standard was externally calibrated against the NIST silicon standard (reference material 640a) to be a = 7.8581(1) Å. This value was held constant in all subsequent Rietveld refinements, allowing an appropriate correction for zero-point shift and sample displacement in each data set. The Rietveld analyses were carried out assuming the structural models of erionite and offretite from Gard and Tait (1973) and Alberti et al. (1996), respectively. A Chebyshev polynomial function with 6–9 coefficients was used to model the background. Bragg peak profiles were modeled by an asymmetric pseudo-Voigt function with three refinable coefficients. Independent peak profile coefficients were refined for each phase, including the internal standard. In several experiments, the hand-separated material was found to contain a significant amount of impurity phases, mainly levyne. When the impurity level was higher than

TABLE 2. Chemical composition, unit-cell parameters, and optical sign of erionites

Sample No.	1	2	3	4	5	6	7	8	9
SiO_2	54.86	50.46	50.54	48.82	56.56	50.83	49.50	48.99	49.83
Al_2O_3	15.21	18.96	18.50	18.30	15.75	18.47	19.61	19.05	19.39
Fe_2O_3	0.21	0.04	tr.	tr.	0.07	tr.	tr.	tr.	tr.
MgO	0.56	0.35	0.47	0.04	1.15	0.14	0.32	0.05	0.41
CaO	5.46	1.68	7.48	7.75	4.70	7.32	6.99	0.77	6.86
SrO	0.03	0.13	0.03	0.06	0.08	0.16	0.04	tr.	0.10
BaO	0.02	0.15	0.05	0.07	0.01	0.06	0.11	0.08	0.03
Na_2O	0.03	5.40	0.10	0.21	0.19	0.20	0.78	6.38	0.80
K_2O	2.78	4.30	3.37	3.43	2.89	3.34	3.19	5.21	3.12
H_2O	20.84	18.53	19.46	21.32	18.60	19.47*	19.47*	19.47*	19.47*
Si	27.18	25.07	25.14	24.97	27.18	25.27	24.67	24.83	24.79
Al	8.88	11.11	10.85	11.03	8.92	10.82	11.52	11.37	11.37
Fe	0.08	0.01	—	—	0.02	—	—	—	—
Mg	0.41	0.26	0.35	0.03	0.82	0.10	0.24	0.04	0.31
Ca	2.90	0.89	3.99	4.25	2.42	3.90	3.73	0.42	3.65
Sr	0.01	0.04	0.01	0.02	0.02	0.05	0.01	—	0.03
Ba	—	0.03	0.01	0.01	—	0.01	0.02	0.02	0.01
Na	0.03	5.20	0.10	0.21	0.18	0.19	0.75	6.27	0.77
K	1.76	2.73	2.14	2.24	1.77	2.12	2.03	3.37	1.98
H_2O	34.43	30.71	32.28	36.36	29.82	32.29	32.36	32.90	32.31
Number of points	9	6	9	13	8	6	7	7	8
E%	+5.3	+7.1	−1.0	−0.4	+5.3	+3.7	+6.8	+7.5	+5.9
R	0.75	0.69	0.70	0.69	0.75	0.70	0.68	0.69	0.69
M/(M+D)	0.35	0.87	0.34	0.36	0.37	0.36	0.41	0.95	0.41
Ca/D	0.87	0.73	0.92	0.99	0.74	0.96	0.93	0.88	0.91
Na/M	0.02	0.66	0.04	0.09	0.09	0.08	0.27	0.65	0.28
a (Å)	13.310(1)	13.320(1)	13.333(1)	13.339(1)	13.289(1)	13.336(1)	13.338(1)	13.321(1)	13.330(1)
c (Å)	15.070(3)	15.186(2)	15.091(2)	15.112(2)	15.079(2)	15.084(3)	15.126(2)	15.194(2)	15.174(4)
V (Å³)	2312.1(5)	2333.4(4)	2323.3(5)	2328.8(4)	2306.2(4)	2323.0(5)	2330.4(4)	2334.8(4)	2335.1(6)
Optical sign	±	−	−	−	±	−	−	+	−

Note: EMPA analyses were renormalized using the water content measured by thermal gravimetric analysis or using a theoretical estimate based on the grand mean values of erionite samples (*). Atomic ratios are based on the cell of 72 framework O atoms. The balance error (E%) is defined in Equation 1 as $100 \times [(Al + Fe)_{ob} - Al_{th}]/Al_{th}$, where $Al_{th} = Na + K + 2 \times (Ca + Mg + Sr + Ba)$ (Passaglia 1970). M = Na + K; D = Ca + Mg + Sr + Ba.

TABLE 2—*Continued*

Sample No.	10	11	12	13	14	15	16	17	18
SiO_2	49.29	50.44	57.75	53.82	49.00	51.96	54.99	50.72	53.51
Al_2O_3	19.44	19.53	15.12	16.60	19.48	17.20	15.36	18.61	16.36
Fe_2O_3	tr.	0.43	0.04	0.10	tr.	0.03	0.10	0.02	tr.
MgO	0.68	0.50	0.74	0.10	0.55	0.20	0.10	0.57	0.05
CaO	7.70	2.55	4.72	7.17	8.15	6.25	2.41	7.06	6.55
SrO	0.08	tr.	tr.	0.03	0.07	0.58	0.26	0.05	0.12
BaO	0.08	0.04	0.04	0.09	0.09	0.06	0.07	0.02	0.02
Na_2O	0.15	5.77	0.16	0.06	0.14	0.26	3.14	0.29	0.31
K_2O	3.10	3.91	3.32	2.70	3.04	3.06	4.10	3.18	2.56
H_2O	19.47*	16.83	18.11	19.33	19.47*	20.40	19.47*	19.47*	20.52
Si	24.58	24.63	27.59	26.41	24.47	26.00	27.15	25.16	26.57
Al	11.42	11.24	8.51	9.60	11.47	10.14	8.94	10.88	9.57
Fe	—	0.16	0.01	0.04	—	0.01	0.04	0.01	—
Mg	0.51	0.36	0.53	0.07	0.41	0.15	0.07	0.42	0.04
Ca	4.11	1.33	2.42	3.77	4.36	3.35	1.27	3.75	3.48
Sr	0.02	—	—	0.01	0.02	0.17	0.08	0.01	0.04
Ba	0.02	0.01	0.01	0.02	0.02	0.01	0.01	—	—
Na	0.15	5.46	0.15	0.06	0.14	0.25	3.01	0.28	0.30
K	1.97	2.44	2.02	1.69	1.94	1.95	2.58	2.01	1.62
H_2O	32.37	27.41	28.86	31.63	32.43	34.04	32.06	32.21	33.98
Number of points	8	7	12	24	11	9	8	10	9
E%	−0.2	−0.5	+5.2	+1.2	−2.0	+6.1	+6.1	+2.0	+5.9
R	0.68	0.69	0.76	0.73	0.68	0.72	0.75	0.70	0.74
M/(M+D)	0.31	0.82	0.42	0.31	0.30	0.37	0.80	0.35	0.35
Ca/D	0.88	0.78	0.82	0.97	0.91	0.91	0.89	0.90	0.98
Na/M	0.07	0.69	0.07	0.03	0.07	0.11	0.54	0.12	0.16
a (Å)	13.344(1)	13.331(1)	13.264(1)	13.304(1)	13.345(1)	13.316(1)	13.277(1)	13.340(1)	13.311(1)
c (Å)	15.128(4)	15.220(3)	15.067(1)	15.078(3)	15.124(3)	15.095(2)	15.124(3)	15.110(2)	15.067(2)
V (Å³)	2332.8(6)	2342.5(5)	2295.7(3)	2311.0(6)	2332.6(5)	2317.8(4)	2308.7(4)	2328.5(4)	2311.8(2)
Optical sign	−	−	+	−	−	−	+	−	−

TABLE 2—*Continued*

	19	20	21	22	23	24	25
SiO_2	49.08	56.84	51.67	55.26	53.54	50.31	58.35
Al_2O_3	19.37	13.87	17.97	14.60	16.76	17.52	13.32
Fe_2O_3	tr.	0.04	0.02	0.81	0.06	0.02	0.16
MgO	1.12	0.08	0.47	0.78	0.10	0.08	0.83
CaO	6.95	1.87	6.72	2.71	4.27	4.63	4.11
SrO	0.35	tr.	tr.	tr.	0.03	0.04	tr.
BaO	0.21	0.12	0.05	0.04	0.06	0.03	0.68
Na_2O	0.03	2.42	0.30	2.83	2.79	3.39	0.36
K_2O	3.42	5.28	3.32	3.37	3.46	3.31	2.72
H_2O	19.47*	19.47*	19.47*	19.60	18.93	20.67	19.47*
Si	24.54	28.01	25.57	27.21	26.32	25.49	28.31
Al	11.41	8.05	10.48	8.48	9.71	10.46	7.61
Fe	—	0.02	0.01	0.30	0.02	0.01	0.06
Mg	0.83	0.06	0.35	0.57	0.07	0.06	0.60
Ca	3.72	0.99	3.57	1.43	2.25	2.51	2.14
Sr	0.10	—	—	—	0.01	0.01	—
Ba	0.04	0.02	0.01	0.01	0.01	0.01	0.13
Na	0.03	2.31	0.29	2.70	2.66	3.33	0.34
K	2.18	3.32	2.10	2.12	2.17	2.14	1.68
H_2O	32.47	31.99	32.14	32.19	31.04	34.93	31.50
Number of points	8	10	7	8	9	9	8
E%	−1.7	+3.8	+2.5	−4.1	+2.1	−1.8	−0.9
R	0.68	0.78	0.71	0.76	0.73	0.71	0.79
M/(M+D)	0.32	0.84	0.38	0.71	0.67	0.68	0.41
Ca/D	0.79	0.92	0.91	0.71	0.96	0.97	0.75
Na/M	0.01	0.41	0.12	0.56	0.55	0.61	0.17
a (Å)	n.d.	13.227(1)	13.338(1)	n.d.	13.290(1)	13.312(1)	13.233(1)
c (Å)	n.d.	15.075(3)	15.100(2)	n.d.	15.132(2)	15.162(2)	15.055(4)
V (Å^3)	n.d.	2284.0(4)	2326.2(4)	n.d.	2314.7(3)	2326.8(4)	2283.1(6)
Optical sign	−	+	−	+	−	−	+

TABLE 3. Chemical composition, unit-cell parameters, and optical sign of offretites

	1	2	3	4	5	6	7	8	9
SiO_2	51.42	50.63	52.96	51.30	54.59	53.60	50.62	51.32	51.92
Al_2O_3	19.54	18.57	17.23	18.56	16.20	17.00	19.25	18.49	18.09
Fe_2O_3	tr.	0.40	0.06	tr.	0.02	0.05	0.03	0.02	0.02
MgO	3.13	2.78	1.97	2.89	2.05	2.32	3.21	2.69	2.88
CaO	3.80	4.22	2.60	3.49	3.56	3.90	4.01	4.17	3.67
SrO	0.16	0.10	tr.	0.38	0.02	tr.	0.03	tr.	0.08
BaO	0.05	0.77	0.04	0.12	0.11	0.09	0.08	0.02	0.07
Na_2O	0.04	tr.	1.52	0.08	0.24	0.07	0.02	0.04	tr.
K_2O	2.98	2.68	3.76	3.34	3.36	3.12	2.91	3.41	2.79
H_2O	18.88	19.85*	19.85*	19.85*	19.85*	19.85*	19.85*	19.85*	20.48
Si	12.49	12.55	13.05	12.66	13.36	13.12	12.46	12.65	12.81
Al	5.60	5.43	5.01	5.40	4.67	4.91	5.58	5.37	5.26
Fe	—	0.08	0.01	—	—	0.01	0.01	—	—
Mg	1.13	1.03	0.73	1.06	0.75	0.85	1.18	0.99	1.06
Ca	0.99	1.12	0.69	0.92	0.93	1.02	1.06	1.10	0.97
Sr	0.02	0.01	—	0.05	—	—	—	—	0.01
Ba	0.01	0.08	—	0.01	0.01	0.01	0.01	—	0.01
Na	0.02	—	0.73	0.04	0.11	0.03	0.01	0.02	—
K	0.92	0.85	1.18	1.05	1.05	0.97	0.91	1.07	0.88
H_2O	15.30	16.41	16.32	16.33	16.20	16.21	16.29	16.32	16.85
Number of points	8	6	10	13	11	12	10	11	7
E%	+6.9	+3.5	+5.8	+4.1	+2.7	+3.2	+3.3	+2.1	+5.6
R	0.69	0.70	0.72	0.70	0.74	0.73	0.69	0.70	0.71
M/(M+D)	0.30	0.28	0.57	0.35	0.41	0.35	0.29	0.34	0.30
Ca/D	0.46	0.50	0.49	0.45	0.55	0.54	0.47	0.53	0.47
Na/M	0.02	0.00	0.38	0.04	0.09	0.03	0.01	0.02	0.00
a (Å)	13.315(2)	13.289(3)	13.267(2)	13.294(4)	13.277(3)	13.278(2)	13.319(3)	13.300(3)	13.293(2)
c (Å)	7.598(2)	7.588(2)	7.583(2)	7.571(3)	7.592(2)	7.587(2)	7.604(2)	7.594(2)	7.608(3)
V (Å^3)	1166.7(4)	1160.6(6)	1156.1(4)	1158.9(9)	1159.0(5)	1158.4(5)	1168.3(6)	1163.4(5)	1164.3(8)
Optical sign	−	−	+	±	+	+	−	?	±

Note: Results of the EMPA analyses have been renormalized using the water content measured by thermal gravimetric analysis or using a theoretical estimate based on the grand mean values of offretite samples (*). Atomic ratios are based on the cell of 36 framework O atoms. The balance error (E%) is defined as in Equation 1. M = Na + K; D = Ca + Mg + Sr + Ba.

TABLE 3—*Continued*

	10	11	12	13
SiO_2	51.21	51.10	50.77	50.59
Al_2O_3	18.94	18.57	18.84	18.77
Fe_2O_3	0.02	0.09	0.22	0.04
MgO	2.90	2.77	1.89	2.97
CaO	4.09	4.26	5.66	4.06
SrO	0.24	0.07	0.21	tr.
BaO	0.09	0.03	0.03	0.47
Na_2O	tr.	0.01	0.02	0.06
K_2O	2.68	2.90	2.50	3.20
H_2O	19.85*	20.20	19.85*	19.85*
Si	12.58	12.62	12.54	12.52
Al	5.49	5.41	5.49	5.47
Fe	—	0.02	0.04	0.01
Mg	1.06	1.02	0.70	1.09
Ca	1.08	1.13	1.50	1.08
Sr	0.03	0.01	0.03	—
Ba	0.01	—	—	0.05
Na	—	0.01	0.01	0.03
K	0.84	0.91	0.79	1.01
H_2O	16.27	16.64	16.35	16.39
Number of points	9	27	9	7
E%	+5.6	+3.2	+5.2	+0.2
R	0.70	0.70	0.70	0.70
M/(M+D)	0.28	0.30	0.26	0.32
Ca/D	0.50	0.52	0.67	0.49
Na/M	0.00	0.01	0.01	0.03
a (Å)	13.311(3)	13.309(3)	13.308(5)	13.301(3)
c (Å)	7.604(2)	7.598(2)	7.597(4)	7.594(3)
V (Å³)	1166.8(5)	1165.6(7)	1164.7(9)	1163.5(4)
Optical sign	–	–	±	–

about 4–5 wt%, as visually estimated from the diffraction powder patterns, the impurity phase was inserted as an additional phase in the refinement.

Unit-cell parameters refined by the above procedure are believed to be highly consistent, due to the use of the internal standard. A few samples were measured in both the Bragg-Brentano and Debye-Scherrer geometries, as a check for systematic errors: The refined unit-cell parameters always agreed within 3 esd. Final results are reported in Tables 2 and 3.

Multivariate statistical analysis

The resulting crystallochemical and unit-cell parameters were statistically analyzed by multiple regression procedures to discriminate distinctive chemical parameters for the two zeolites and their possible correlation with the unit-cell parameters. The multivariate analysis was carried out with the widely used Statistical Package for the Social Sciences (SPSS) and a revised version of the stepwise regression program BMD02R (Health Sciences Computing Facility, UCLA). Besides simple chemical variables, the following combined parameters were tested for significant correlation with each other and with the unit-cell parameters: R = Si/(Si + Al); M = Na + K; D = Ca + Mg + Sr + Ba; V1 = M/D; V2 = M/(M + D); V3 = Ca/D; V4 = Na/M; V5 = (Ca/D) + (Na/M). Some of these parameters are reported in Tables 2 and 3. The Araules sample was excluded from the statistical computations because of its ambiguous definition.

RESULTS AND DISCUSSION

Figure 4 shows the present chemical analyses on a diagram similar to the representation of the literature data in Figure 1. The vertical distribution of plotted data represents the variation in the Si/Al ratio of the samples [i.e., R = Si/(Si + Al) increases from 0.67 at the bottom to

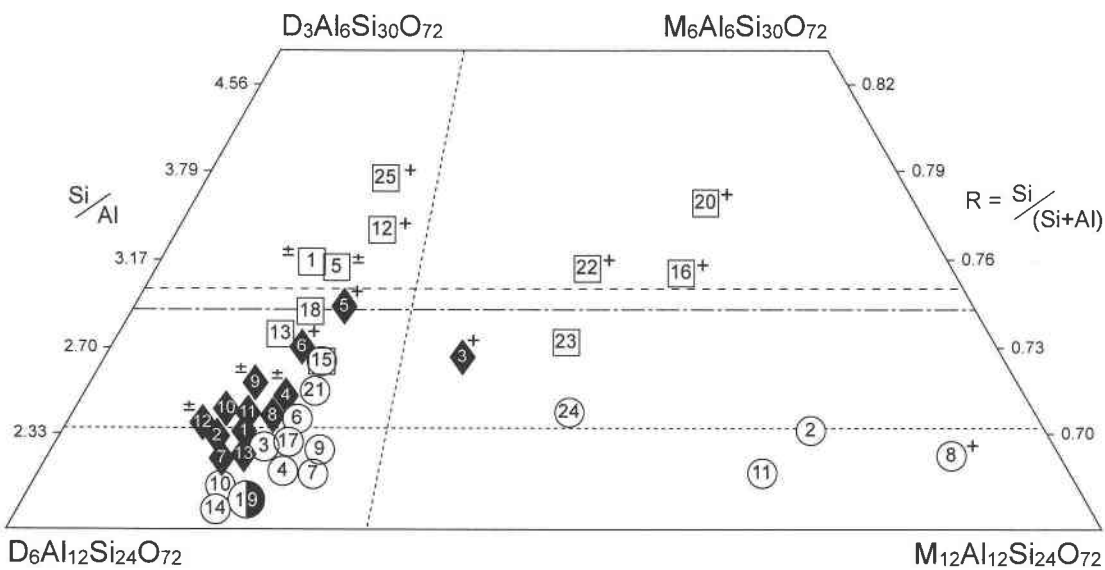

FIGURE 4. Compositional diagram showing the mean chemical analyses of the studied erionite (open circles = erionites associated with levyne; open squares = isolated erionites) and offretite (solid diamonds) samples. The sample numbers correspond to those listed in Table 1. Discrimination lines as in Figure 1. Optical sign of elongation is adjacent to each symbol: No mark means negative elongation sign, (+) means positive elongation sign, (±) means sample with crystals having positive or negative elongation sign (see text for details).

0.83 at the top], whereas the horizontal distribution represents the variation in D/M cation content (i.e., divalent cations only at the left; monovalent cations only at the right). Erionite samples associated with levyne have symbols distinct from those of isolated erionites.

Although the overall distribution of points in Figures 1 and 4 is broadly comparable, the compositional field of the two zeolite species differs in the two diagrams. One major difference is the vertical distribution (i.e., the Si/Al ratio) of the samples. The literature data (Fig. 1) seem to indicate a neat division (at about R = 0.73) with all offretite samples having $R < 0.73$, and all but one erionite samples having $R > 0.73$. This limit is about the average of those proposed for erionite-offretite discrimination by Wise and Tschernich (1976: Si/Al = 3.0 or R = 0.75) and Rinaldi (1976: Si/Al = 2.4 or R = 0.71). The discrimination is not supported by the new chemical analyses (Fig. 4): Both the grand mean value and the observed range of R in erionite and offretite are similar. The statistical mean R value is 0.72(3) and 0.71(2), and observed range is $0.68 < R < 0.79$ and $0.69 < R < 0.74$ in erionite and offretite, respectively.

Two results are apparent: (1) in Si,Al compositional space the crystal-chemical fields of erionite and offretite largely overlap, and there is no discrimination between the two species; (2) The observed R range is extended to larger R values for offretite and to lower R values for erionite, than the data reported in the literature. Consequently, compositional limits based on framework Si/Al ratio cannot be used to discriminate species.

Furthermore, Figure 4 clearly indicates that among the analyzed erionite samples, differences exist in the framework Si/Al content between the levyne-associated (open circles) and the levyne-free (open squares) erionites: The erionite samples epitaxially overgrown on levyne are substantially more Al-rich. Because the average R value of levyne is 0.65(2) (Galli et al. 1981), it is clear that erionite can grow on levyne only by developing a tetrahedral framework with a Si/Al ratio as close as possible to levyne and with an R factor lower than about 0.71. Erionite samples not associated with levyne (Table 1), both isolated (nos. 1, 12, 13, 18, 20) and associated with other zeolites such as analcime (no. 16), phillipsite (no. 23), or heulandite (nos. 5, 22, 25), are invariably more Si-rich. The observed difference is particularly evident in a few samples. In the specimens from nearby localities at Montecchio Maggiore, the erionite associated with levyne (no. 15) has a substantially lower Si/Al ratio that the isolated erionite (no. 16). The same is observed in the samples from Mt. Adamson, Antarctica (nos. 23, 24). All samples but one (no. 1) from Northern Ireland are intimately associated with levyne. No. 1 has a very high Si/Al ratio, whereas other samples from nearby localities are all very Si-poor (nos. 2, 3, and 4).

It is remarkable that no offretite-levyne intergrowth was observed during the present investigation. In contrast, erionite was commonly found as an epitaxial overgrowth on levyne lamellae. On the basis of our results, several reports of offretite-levyne intergrowths in the literature, e.g., the samples from Douglas Lake Rd. (no. 6), Beech Creek (no. 14), and all of the Australian occurrences (nos. 7–11) reported in Table 1, have been proven to be misidentified and erionite is the species present. In this light, the other occurrences of offretite on levyne (Wise and Tschernich 1976; Rídkošil and Danek 1983; Kile and Modreski 1988) should be considered dubious. Instead offretite is found as an epitaxial overgrowth on chabazite (Passaglia and Tagliavini 1994; Passaglia et al. 1996).

Erionite and offretite are not distinguishable on the basis of the optical elongation sign, as originally proposed by Sheppard and Gude (1969), although this method has become a routine tool for identification. All erionite and offretite samples in the lowermost part of Figure 4 essentially have a negative elongation sign, independent of the mineral species, whereas most samples having $R > 0.74$ have a positive elongation sign. In the case of erionite, the elongation sign is negative in samples having $R \leq 0.74$, positive in samples having $R \geq 0.76$, and positive or negative depending on the particular crystal investigated in samples having intermediate R values. In the case of offretite, the elongation sign is negative in samples having $R \leq 0.70$, positive in samples having $R \geq 0.72$, and again positive or negative depending on the particular crystal investigated in samples having R values close to 0.71. Therefore, optical investigation is not conclusive for identification purposes because the observed sign of elongation in erionite and offretite depends on the Si/Al content in the zeolite framework. The earlier observations of Sheppard and Gude (1969) were biased by the presence of many Si-rich "sedimentary" erionites among the analyzed samples. Erionites diagenetically formed by alteration of volcanic glass are invariably Si- and Na-rich, and therefore commonly show positive optical sign of elongation. Optical properties alone, when not supported by adequate X-ray or electron diffraction characterization, cannot be used for erionite-offretite discrimination. The purely optical method is the origin of many misdefined samples in the literature.

The proposed discrimination based on the D/M cation ratio (Sheppard and Gude 1969: D = M compositional limit plotted as a dotted sub-vertical line in Figs. 1 and 4) is also not applicable. Figure 4 clearly shows that most of the analyzed samples, whether erionite or offretite, plot on the leftmost part of the diagram, that is in most samples the divalent cation content is significantly larger than the monovalent cation content.

The compositional diagram based on the extraframework cation content of the studied samples is shown in Figure 5. Although the analogous diagram showing the literature data presents a rather confused picture (Fig. 2), the present erionite and offretite samples plot in well-defined compositional fields. All points are located in a limited region in terms of (K + Sr + Ba) variation, whereas there is a large distribution (and discrimination) in terms of Mg/(Ca + Na) ratio.

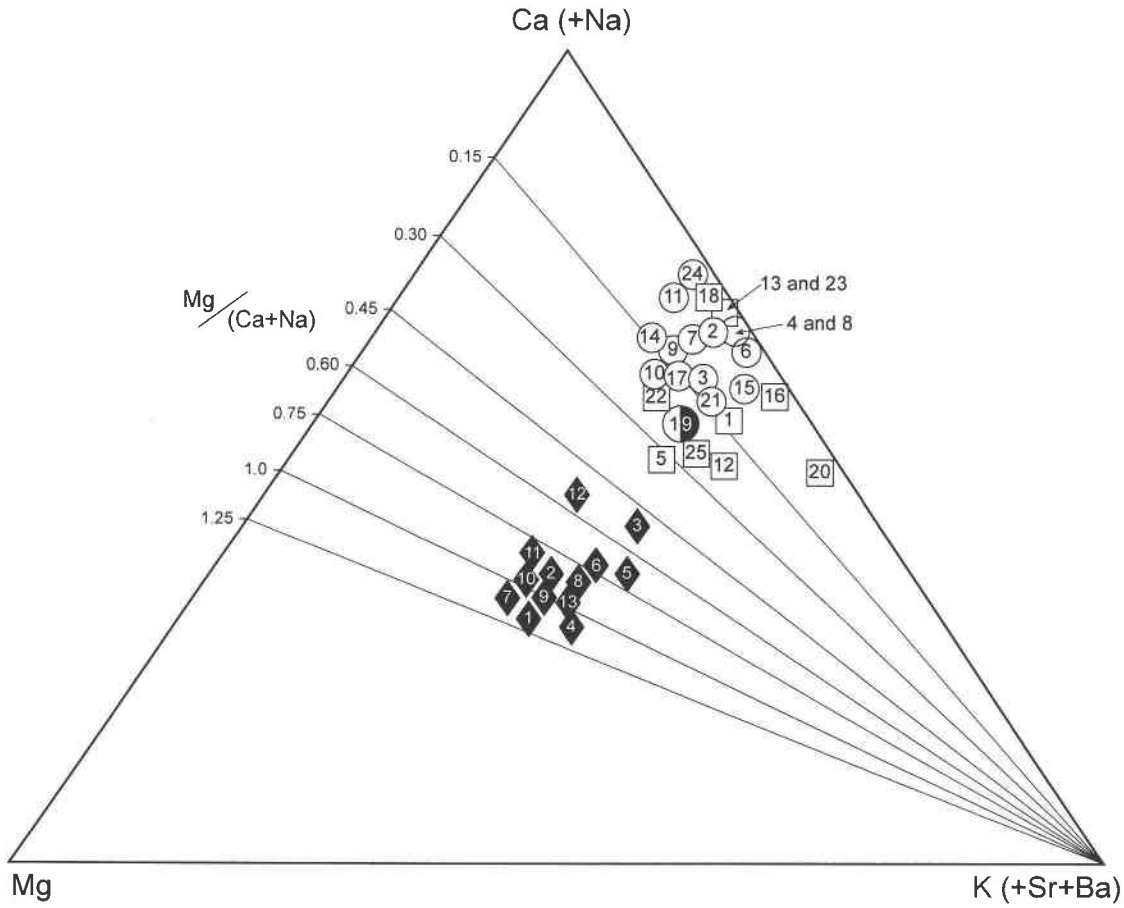

FIGURE 5. Compositional diagram showing the extraframework cation content of studied erionite and offretite samples. Symbols as in Figure 4.

The narrow (K + Sr + Ba) distribution is due to the nearly invariant K content and negligible Sr and Ba contents in most samples. As shown by the available structure models, this restriction is clearly due to the fact that the K atoms in both structures are located in the cancrinite cage, and the average K content shown by the chemical analysis is very close to the one required for full occupancy of the crystallographic site at the center of the cancrinite cage.

The most significant discrimination between erionite and offretite is based on the Mg/(Ca + Na) cation ratio, with offretites showing values close to 1.0, and erionites showing values significantly less than 0.3. It is not straightforward to interpret the possible crystal chemical role of Mg on the basis of the crystal structural models. However, the observed chemical discrimination clearly shows that the Mg/(Ca + Na) cation ratio might well be a major controlling factor influencing the crystallization of offretite in place of erionite, in the presence of similar Si,Al activities in the circulating fluids. All Mg, Ca, and Na cations, and at times excess K cations, are located in the large zeolitic cages of the two structures. Only one type of cage is present in erionite (the 23-hedron or erionite cage), whereas two different cavities are present in offretite (the 14-hedron or gmelinite cage; and the large channels formed by 12-membered rings of tetrahedra). A detailed structural study carried out to elucidate the problem (Gualtieri et al. 1998) seem to indicate that the ability of offretite to host a large amount of octahedrally coordinated Mg cations is related to the presence of several structurally different large openings and therefore related to the availability of various extraframework cation sites.

Clear distinction of the erionite and offretite compositional fields shown in Figure 5 also indicates that erionite-offretite intergrowths are very uncommon in natural samples, at least in large amounts. Faulted sequences containing domains of the two zeolites or high stacking-defect densities have been reported in the literature (Kokotailo et al. 1972; Bennett and Grose 1976; Rinaldi 1976) and are certainly possible. However, if most occurrences consisted of a mixture of the two phases, it is to be expected that many samples would fall between the two described compositional fields. Rarity of erionite-offretite intergrowths is also supported by the fact that all the investigated samples present a high degree of chemical homogeneity. This is clearly impossible should the

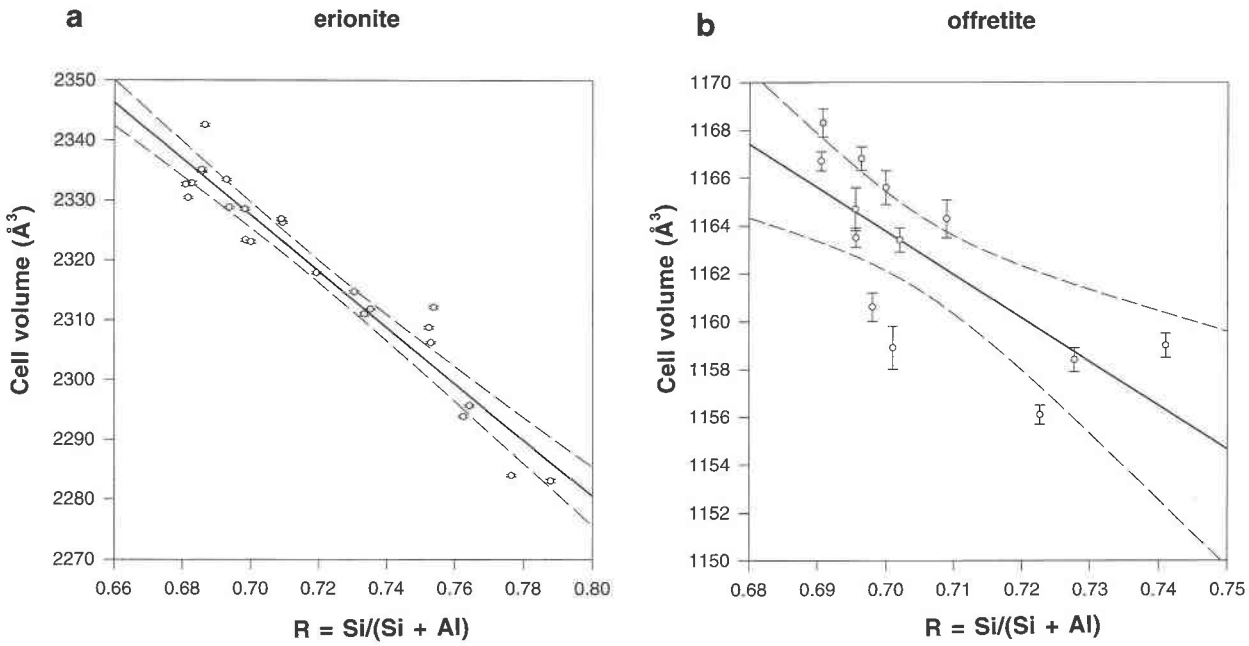

Figure 6. Correlation between the unit-cell volume and the R = Si/(Si + Al) ratio in the framework of (**a**) erionite and (**b**) offretite. The regression curve fit is marked with a thick line, and the dashed lines show the 95% regression confidence level.

individual crystals present different amounts of the two phases.

Presence of a small quantity of intergrowths, below the detection limit of the X-ray powder diffraction technique, might be present in the samples located at the boundary of the compositional fields, i.e., in Mg-poor offretites or in Mg-rich erionites. This possibility was thoroughly checked in several samples using transmission electron microscopy (Gualtieri et al. 1998), and the results were negative in all cases except for the anomalous erionite sample from Araules (no. 19).

Statistical analysis using multivariate regression techniques indicates that no significant correlations exist among the chemical parameters pertaining to each zeolite, and the only significant correlation among the crystallographic parameters is the expected large influence of the unit-cell parameter *a* on the unit-cell volume, both in erionite and in offretite (correlation factors 0.92 and 0.95, respectively). In comparison, the correlation factors between the unit-cell parameter *c* and the unit-cell volume are below 0.8 in both zeolites, showing that the structures are relatively rigid along the major symmetry axis.

A good correlation was also found between the composition of the framework tetrahedra (expressed in terms of the Si/Al or the R ratios) and the unit-cell volume. The correlation is excellent in erionite (Fig. 6a: correlation factor 0.96), and poorer in offretite (Fig. 6b: correlation factor 0.72), in part because the erionite R compositional range is much broader.

Because the framework expansion produced by the introduction of the Al atoms has almost no influence on the *c* axis of erionite and is linked to the elongation of the *a* axis (as shown by the good *a* vs. volume correlation), the Al atoms in erionite are expected to preferentially enter the T2 framework tetrahedral site, forming the single six-membered rings that connect the columns formed by the cancrinite cages and the double hexagonal rings. The correlation between the Al content and the unit-cell volume (or the *a* unit-cell parameter) in erionite is statistically significant, and it is possible to reliably estimate the R ratio in the erionite framework from the measured crystallographic lattice parameters, on the basis of the regression equation:

$$R = Si/(Si + Al) = -0.00213 \times V + 5.65149 \quad (3)$$

The same correlation is present in offretite although it is much less significant, leading to the speculation that the Al atoms should be essentially disordered on the framework sites in offretite, in agreement with the conclusions of Alberti et al. (1996).

Conclusions

The resulting average crystal-chemical formulae representative of the two zeolites:

erionite $Ca_3K_2Na_2[Al_{10}Si_{26}O_{72}]\cdot 30H_2O$ $Z = 1$

offretite $CaKMg[Al_5Si_{13}O_{36}]\cdot 16H_2O$ $Z = 1$

are different from those commonly accepted and reported, for example, in Gottardi and Galli (1985).

Both zeolites show large variation in framework Si/Al ratio and extraframework cation content. Erionite shows a wider range in Si/Al ratio than offretite, especially when it is associated with levyne. Large cation variations in

erionite are best described using the Ca/Na ratio. The cation content of offretite has very limited variation, and the Ca/Mg ratio is always very close to 1.0.

Acknowledgments

Italian MURST and CNR are acknowledged for financial support. W.D. Birch, M. Boscardin, H. Foy, Z. Gabelica, and F. Saccardo kindly made samples available for the investigation. G. Vezzalini and S. Bigi performed the chemical analyses on the ARL-SEMQ electron microprobe analyzer at the Università di Modena. M. Bertacchini helped with the graphics of chemical diagrams. D.L. Bish, R. Downs, and an anonymous reviewer are thanked for detailed suggestions and improvement of the manuscript.

References cited

Alberti, A., Cruciani, G., Galli, E., and Vezzalini, G. (1996) A reexamination of the crystal structure of the zeolite offretite. Zeolites, 17, 457–461.

Batiashvili, T.V. and Gvakhariya, G.V. (1968) Erionite found for the first time in Georgia. Doklady of the Russian Academy of Sciences: Earth Science Sections, 179, 122–124.

Belitskiy, I.A. and Bukin, G.V. (1968) First find of erionite in the U.S.S.R. Doklady of the Russian Academy of Sciences: Earth Science Sections, 178, 103–106.

Bennett, J.M. and Gard, J.A. (1967) Non-identity of the zeolites erionite and offretite. Nature, 214, 1005–1006.

Bennett, J.M. and Grose, R.W. (1978) Characterization of the offretite-levynite intergrowth from Beech Creek, Oregon, by adsorption and electron diffraction. In L.B. Sand and F.A. Mumpton, Eds., Natural Zeolites: Occurrence, Properties, Use, p. 77–83. Pergamon Press, Oxford.

Betz, V. and Hentschel, G. (1978) Offretit und Erionit von Gedern (Vogelsberg). Geologisches Jahrbuch Hessen, 106, 419–421.

Birch, W.D. (1987) Zeolites from Jindivick, Victoria. Australian Mineralogist, 2, 15–19.

———(1988) Zeolites from Phillip Island and Flinders, Victoria. The Mineralogical Record, 19, 451–460.

———(1989) Chemistry of Victorian zeolites. In W.D. Birch, Ed., Zeolites of Victoria, p. 91–102. Mineralogical Society of Victoria Special Publication, 2.

Boles, J.R. and Surdam, R.C. (1979) Diagenesis of volcanogenic sediments in a Tertiary saline lake; Wagon Bed Formation, Wyoming. American Journal of Science, 279, 832–853.

England, B.M. and Ostwald, J. (1979) Levyne-offretite intergrowths from Tertiary basalts in the Merriwa district, Hunter Valley, New South Wales, Australia. Australian Mineralogist, 25, 117–119.

Galli, E., Rinaldi, R., and Modena, C. (1981) Crystal chemistry of levynes. Zeolites, 1, 157–160.

Gard, J.A. and Tait, J.M. (1972) The crystal structure of the zeolite offretite, $K_{1.1}Ca_{1.1}Mg_{0.7}[Si_{12.8}Al_{5.2}O_{36}]\cdot 15.2\ H_2O$. Acta Crystallographica, B28, 825–834.

———(1973) Refinement of the crystal structure of erionite. In J.B. Uytterhoeven, Ed., Proceedings of the Third International Conference on Molecular Sieves, p. 94–99. Leuven University Press, Leuven.

Giovagnoli, L. and Boscardin, M. (1979) Ritrovamento di levyna ed erionite a Montecchio Maggiore (Vicenza). Rivista Mineralogica Italiana, 1, 44–45.

Gottardi, G. and Galli, E. (1985) Natural zeolites, p. 200–214. Springer-Verlag, Berlin Heidelberg.

Gualtieri, A., Passaglia, E., Bigi, S., Viani, A., Artioli, G., and Hanson, J.C. (1998) Crystal structure-crystal chemistry relationships in the zeolites erionite and offretite. American Mineralogist, 83, 590–606.

Gude, A.J. and Sheppard, R.A. (1981) Woolly erionite from the Reese River zeolite deposit, Lander County, Nevada, and its relationship to other erionites. Clays and Clay Minerals, 29, 378–384.

Harada, K., Iwamoto, S., and Kihara, K. (1967) Erionite, phillipsite and gonnardite in the amygdales of altered basalt from Mazé, Niigata Prefecture, Japan. American Mineralogist, 52, 1785–1794.

Hentschel, G. (1980) Weitere Offretit-Vorkommen im Vogelsberg (Hessen). Geologisches Jahrbuch Hessen, 108, 171–176.

———(1986) Paulingit und andere Seltene Zeolithe in einem gefritteten Sandsteineinschluss im Basalt von Ortenberg (Vogelsberg). Geologisches Jahrbuch Hessen, 114, 249–256.

Hentschel, G. and Schricke, W. (1976) Offretit von Geilshausen (Vogelsberg, Hessen). Geologisches Jahrbuch Hessen, 104, 173–176.

Kawahara, A. and Curien, H. (1969) La structure cristalline de l'érionite. Bulletin de la Société française de Minéralogie et de Cristallographie, 92, 250–256.

Kerr, I.S., Gard, J.A., Barrer, R.M., and Galabova, I.M. (1970) Crystallographic aspects of the co-crystallization of zeolite L, offretite, and erionite. American Mineralogist, 55, 441–454.

Kile, D.E. and Modreski, P.J. (1988) Zeolites and related minerals from the Table Mountain lava flows near Golden, Colorado. The Mineralogical Record, 19, 153–184.

Kokotailo, G.T., Sawruck, S., and Lawton, S.L. (1972) Direct observation of stacking faults in the zeolite erionite. American Mineralogist, 57, 439–444.

Larson, A.C. and Von Dreele, R.B. (1996) GSAS, generalized structure analysis system. Los Alamos National Laboratory, document LAUR 86–748.

Lutterotti, L., Gualtieri, A., and Aldrighetti, S. (1996) Rietveld refinement using Debye-Scherrer film techniques. Materials Science Forum, 228–231, 29–34.

Meier, W.M. and Olson, D.H. (1992) Atlas of zeolite structure types. Zeolites, 12, 449–656.

Noh, J.H. and Kim, S.J. (1986) Zeolites from Tertiary tuffaceous rocks in Yeongil Area, Korea. In Y. Murakami, A. Iijima, and J.W. Ward, Eds., New Developments in Zeolite Science and Technology, p. 59–66. Kodansha-Elsevier, Tokyo-Amsterdam.

Passaglia, E. (1970) The crystal chemistry of chabazites. American Mineralogist, 55, 1278–1301.

Passaglia, E. and Tagliavini, A. (1994) Chabazite-offretite epitaxial overgrowths in cornubianite from Passo Forcel Rosso, Adamello, Italy. European Journal of Mineralogy, 6, 397–405.

———(1995) Erionite from Faedo, Colli Euganei, Italy. Neues Jahrbuch für Mineralogie Monatshefte, 185–191.

Passaglia, E., Galli, E., and Rinaldi, R. (1974) Levynes and erionites from Sardinia, Italy. Contribution to Mineralogy and Petrology, 43, 253–259.

Passaglia, E., Tagliavini, A., and Gutoni, R. (1996) Offretite and other zeolites from Fittà (Verona, Italy). Neues Jahrbuch für Mineralogie Monatshefte, 418–428.

Pongiluppi, D. (1976) Offretite, garronite and other zeolites from "Central Massif," France. Bulletin de la Société française de Minéralogie et de Cristallographie, 99, 322–327.

Rinaldi, R. (1976) Crystal chemistry and structural epitaxy of offretite-erionite from Sasbach, Kaiserstuhl. Neues Jahrbuch für Mineralogie Monatshefte, 145–156.

Rychlý, R., Danek, M., and Siegl, J. (1982) Structural epitaxy of offretite-erionite from Prackovice nad Labem, Bohemia. Chemie der Erde, 41, 263–268.

Rídkošil, T. and Danek, M. (1983) New physical and chemical data for levyne-offretite intergrowths from Zezice, near Ústí nad Labem, Czechoslovakia. Neues Jahrbuch für Mineralogie Abhandlungen, 147, 99–108.

Sameshima, T. (1978) Zeolites in tuff beds of the Miocene Waitamata group, Auckland province, New Zealand. In L.B. Sand and F.A. Mumpton, Eds., Natural Zeolites: Occurrence, Properties, Use, p. 309–317. Pergamon Press, Oxford.

Sheppard, R.A. and Gude, A.J. (1969) Chemical composition and physical properties of the related zeolites offretite and erionite. American Mineralogist, 54, 875–886.

Sheppard, R.A., Gude, A.J., and Munson, E.L. (1965) Chemical composition of diagenetic zeolites from tuffaceous rocks of the Mojave desert and vicinity, California. American Mineralogist, 50, 244–249.

Sheppard, R.A. Gude, A.J., Desborough, G.A., and White, J.S., Jr. (1974) Levyne-offretite integrowths from basalt near Beech Creek, Grant County, Oregon. American Mineralogist, 59, 837–842.

Shimazu, M. and Mizota, T. (1972) Levyne and erionite from Chojabaru, Iki Island, Nagasaki Prefecture, Japan. Journal of the Japanese Asso-

ciation of Mineralogists, Petrologists and Economic Geologists, 67, 418–424.

Staples, L.W. and Gard, J.A. (1959) The fibrous zeolite erionite; its occurrence, unit cell, and structure. Mineralogical Magazine, 32, 261–281.

Surdam, R.C. and Eugster, H.P. (1976) Mineral reactions in the sedimentary deposits of the Lake Magadi region, Kenya. Geological Society of America Bulletin, 87, 1739–1752.

Tschernich, R.W. (1992) Zeolites of the world, 563 p. Geoscience Press Inc., Phoenix, Arizona.

Vezzalini, G., Quartieri, S., Rossi, A., and Alberti, A. (1994) Occurrence of zeolites from Northern Victoria Land (Antarctica). Terra Antartica, 1, 96–99.

Wise, W.S. and Tschernich, R.W. (1976) The chemical compositions and origin of the zeolites offretite, erionite and levyne. American Mineralogist, 61, 853–863.

Manuscript received March 31, 1997
Manuscript accepted December 14, 1997
Paper handled by Ronald C. Peterson